Astron. Astrophys. 302, L25–L28 (1995)

ASTRONOMY AND ASTROPHYSICS

Letter to the Editor

Molecular and atomic fractionation effects in the NGC 1977 molecular cloud

Nigel R. Minchin and Glenn J. White

Department of Physics, Queen Mary and Westfield College, University of London, Mile End Road, London E1 4NS, UK

Received 16 March 1995 / Accepted 12 September 1995

Abstract. The photon-dominated region (PDR) associated with the NGC 1977 molecular cloud has been observed at high resolution in the ^{13}CO and $C^{18}O$ J = 2→1 and the [CI] $^3P_1$–$^3P_0$ lines. The $N(^{13}CO)/N(C^{18}O)$ ratio has been plotted against visual extinction (A_v) and fits a power law relation. The highest values, as expected, occur for observed positions with the lowest derived extinction, with $N(^{13}CO)/N(C^{18}O)$ exceeding the terrestrial value (5.5) for $A_v \leq 60$ magnitudes. In the outermost parts of the cloud ($A_v \leq 20$ magnitudes) the $N(^{13}CO)/N(C^{18}O)$ ratio is largest, up to 20. Comparison with similar observations of the S140 and Orion Bright Bar regions implies that higher incident UV field leads to increased fractionation effects. The $N(CI)/N(CO)$ ratio has been plotted against visual extinction, as derived from $N(C^{18}O)$, for the range A_v=20–100 magnitudes and also fits a power law relation. $N(CI)/N(CO)$ increases with decreasing extinction from ∼0.03–0.04 for A_v ∼100 mags. to ≥0.1 for A_v ∼20 mags., corresponding to positions near the edge of the HII region/molecular cloud interface. Comparison with identical observations of the S140 and Orion Bright Bar regions implies that, unlike $N(^{13}CO)/N(C^{18}O)$, the behaviour of $N(CI)/N(CO)$ is insensitive to incident UV field over this range of extinction.

Key words: stars: early-type – interstellar medium: HII regions – jets and outflows

1. Introduction

The role of incident UV flux on fractionation processes at the irradiated edges of molecular clouds is still unclear. The column density ratio $N(^{13}CO)/N(C^{18}O)$ has been shown to significantly exceed the terrestrial ratio at the edges of several molecular clouds (e.g Frerking *et al.* 1982; Lada et al. 1994). Both selective photodissociation and enhanced ^{13}CO abundance due to ion-molecule exchange reactions have been used to explain the overabundance of ^{13}CO (e.g. van Dishoeck & Black 1988; Turner et al. 1992). Chemical models of molecular cloud interiors predict that almost all the atomic carbon should be locked in CO over timescales of $\sim 10^6$ years, however, large-scale observational studies of several dark clouds imply that the abundance ratio $N(CI)/N(CO)$ is high, not only in the UV irradiated outer envelopes of clouds, but also apparently inside (e.g. Keene et al. 1985; White & Padman 1991). Several mechanisms have been proposed to explain this, including dissociation dur to cosmic ray induced photons following excitation of H_2 by secondary electrons, photodissociation of CO by embedded stars, shock excitation and bistability (e.g. Prasad & Tarafdar 1983; Le Bourlot et al. 1994). However, the large-spatial extent of the [CII] emission observed from molecular clouds, which can only be produced by photodissociation, implies that photon-dominated regions (PDRs) are highly clumpy, allowing UV radiation from external stars to penetrate deep into the cloud interiors before dissociating CO (e.g. Stutzki et al. 1988).

Recent high-resolution observations of S140 and the IRc2/Bright Bar regions of Orion (Minchin, White & Ward-Thompson 1995; White & Sandell 1995), have allowed direct comparison of molecular and atomic line fractionation processes over a large range in extinction (A_v=5–400 mags.). They find significant fractionation effects towards positions with low derived extinction, with the data fitting power law relationships. The values of $N(^{13}CO)/N(C^{18}O)$ observed towards the Bright Bar are systematically higher than observed towards S140 for the same extinction. The fact that the Bright Bar has a higher incident UV field ($\sim 10^5 G_o$) than S140 ($\sim 150 G_o$) imply the increased fractionation may be due to more rapid photodissociation of the optically thinner isotope, $C^{18}O$. $N(CI)/N(CO) \geq 1$ for A_v∼5-10 mags. in both S140 and the IRc2/Bright Bar regions of Orion, with the data fitting similar power law relationships in both regions. This may imply that, unlike the $N(^{13}CO)/N(C^{18}O)$ ratio, $N(CI)/N(CO)$ is not a function of the incident radiation field.

Clearly observations of just two regions are not sufficient to allow firm conclusions. For this reason we have undertaken a detailed study of another archetypical edge-on PDR, that adjacent to the NGC1977 HII region. Extended ^{12}CO and ^{13}CO emission was first observed from this region by Kutner, Evans & Tucker (1976) and revealed a steep drop-off at the HII region/molecular cloud interface. The region has subsequently been mapped in isotopic CO lines (e.g. Kutner et al. 1985), CI line emission (Wootten et al. 1982), CII line emission (Howe et al. 1991) and near and far-infrared continuum emission (Makinen et al. 1985). The dust emission implies the B1 V star HD 37018 (42 Ori) is the only significant energy source for the region (Makinen et al. 1985).

Send offprint requests to: Nigel R. Minchin

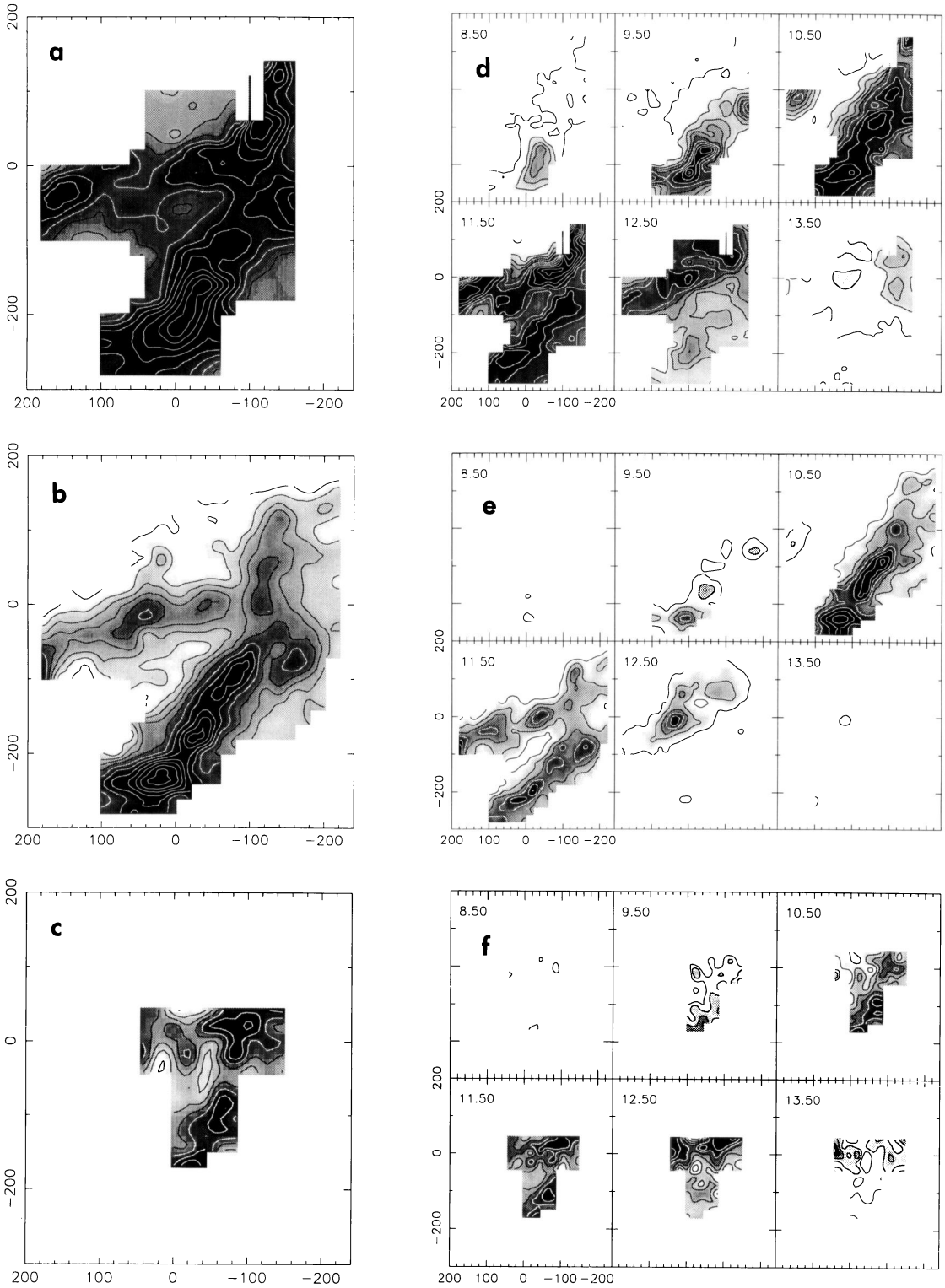

Fig. 1. Greyscale images, with isophotal contour overlayed, of the total integrated intensity between 8 and 14 km s^{-1} for (a) The ^{13}CO J = 2→1 line. The base level contour is 1.5 K-km s^{-1} (3σ) and the contour interval is 9σ. (b) The $C^{18}O$ J = 2→1 line. The base level contour is 2.1 K-km s^{-1} (3σ) and the contour interval is 3σ. (c) The [CI] $^3P_1$–$^3P_0$ line. The base level contour is 13 K-km s^{-1} (6σ) and the contour interval is 2σ. Also shown are velocity channel maps of the integrated intensity for (d) The ^{13}CO J = 2→1 line. The base level contour is 0.6 K-km s^{-1} (3σ) and the contour interval is 9σ. (e) The $C^{18}O$ J = 2→1 line. The base level contour is 1 K-km s^{-1} (3σ) and the contour interval is 9σ. (f) The [CI] $^3P_1$–$^3P_0$ line. The base level contour is 2.7 K-km s^{-1} (3σ) and the contour interval is 2σ. The channel width is 1 km s^{-1}, with the central velocity of the channel indicated in the top left-hand corner of each map. The offsets are in arcseconds from the map centre

2. Observations

All observations were carried out at the James Clerk Maxwell Telescope[1] (JCMT), located on Mauna Kea, Hawaii and were obtained in October 1993 ($C^{18}O$ J = 2→1 line), July 1994 (^{13}CO J = 2→1 line) and July 1995 ([CI] $^3P_1$–$^3P_0$ line). The receivers used were A2 (205–285 GHz) and C2 (450–505 GHz), both single channel SIS mixer systems, used in conjunction with a digital autocorrelation spectrometer (DAS) with 2048 channels. The telescope was operated in position switching mode, with an off-source reference 10 arcmin to the north. Tracking and pointing were consistently within an rms accuracy of 1–2 arcsec. The line observations presented in this paper have been calibrated in units of corrected main-beam brightness temperature $T_{\rm mb}$ ($= T_{\rm A}^*/\eta_{\rm mb}$) and as such have been corrected for all atmospheric, ohmic, scattering and spillover losses. The values of $\eta_{\rm mb}$ were derived using observations of Mars and were 0.68±0.01 for the ^{13}CO and $C^{18}O$ observations and 0.43±0.07 for the atomic carbon observations.

The centre position (0,0) for each of the maps is α_{1950} = $5^h\ 32^m\ 47^s$, δ_{1950} = -4° 58′ 11″. The ^{13}CO J = 2→1 line (220.3987 GHz) map consists of 255 spectra obtained with a grid spacing of one beamwidth (The effective beamwidth for observations at this frequency is ∼20 arcsec). The $C^{18}O$ J = 2→1 line (219.5603 GHz) map consists of 379 spectra also obtained with a grid spacing of mainly one beamwidth, but with additional spectra obtained at a half-beamwidth spacing for positions towards the northern edge of the mapped area, the HII region/molecular cloud interface region. We obtained 70 [CI] $^3P_1$–$^3P_0$ line (492.1622 GHz) spectra at various positions coincident with those mapped in the ^{13}CO and $C^{18}O$ lines.

3. Results

Figure 1 shows greyscale images of the total integrated intensity and velocity channel maps between 8 and 14 km s^{-1} for the ^{13}CO and $C^{18}O$ J = 2→1 lines and the [CI] $^3P_1$–$^3P_0$ line. The morphology delineated by the total integrated emission is similar for all three lines (Figs. 1a, b and c), forming a V shape, with the apex around -100 arcsec to the west of the map centre. Both arms of the V are composed of numerous clumps, with good positional agreement for the isotopic maps and with the southern arm being most prominent. The channel maps (Figs. 1d, e and f) imply close positional coincidence for the clumpy structure within each of the velocity channels. It is also clear that the southern arm is prominent in emission that is blueshifted from the ambient molecular cloud (11-12 km s^{-1}), whilst the northern arm is prominent in redshifted emission. This may imply the southern arm is on the front edge of the molecular cloud, with the northern arm situated on the back edge. The fact that the arms are offset implies that we are not viewing the region as an exact edge-on geometry, but that the illuminating star is closer towards the observer than the observed molecular cloud edge. The observed region is actually only a relatively small part of the elongated ridge of CO emission that extends southeast-northwest (Kutner et al. 1976), with the HII region and illuminating star located to the northeast (e.g. Makinen et al. 1985).

[1]The JCMT is operated by the Royal Observatory, Edinburgh, on behalf of the Particle Physics and Astronomy Research Council, the Netherlands Organisation for Pure Research, and the National Research Council of Canada.

4. Discussion

4.1. $^{13}CO/C^{18}O$ fractionation

To test for the presence of fractionation effects towards the NGC 1977 PDR region, we have used our $C^{18}O$ and ^{13}CO J = 2→1 line data to derive the isotopic column densities, and hence $N(^{13}CO)/N(C^{18}O)$. The equations used are derived from the general equation for column density and are analogous to those used for the J = 3→2 lines (Minchin, White & Ward-Thompson 1995). Both isotopomers are assumed to have the same excitation temperature, which we derived from the ^{12}CO J = 3→2 line peak main beam antenna temperatures. The canonical abundances of ^{13}CO and $C^{18}O$ relative to ^{12}CO are assumed to be 70 and 500 respectively (e.g. Langer & Penzias 1990; Gierens et al. 1992). We have applied the correction factor $\beta = \tau/(1 - e^{-\tau})$, where τ is the line optical depth.

Using the relationship between $N(C^{18}O)$ and A_v derived by Lada *et al* (1994), we have plotted $N(^{13}CO)/N(C^{18}O)$ against extinction for the NGC 1977 PDR region. This is shown in Figure 2. The best fit power law is $N(^{13}CO)/N(C^{18}O) = 28A_v^{-0.4}$, with a correlation coefficient of 0.6. Also plotted are the fits obtained for the S140 and Orion Bright Bar regions (Minchin, White & Ward-Thompson 1995; White & Sandell 1995) over the same extinction range. It should be noted that the Lada et al. relationship was only derived for $A_v \leq 15$ mags., so our extrapolation to higher values may lead to slight inaccuracies, although this will not affect our conclusions.

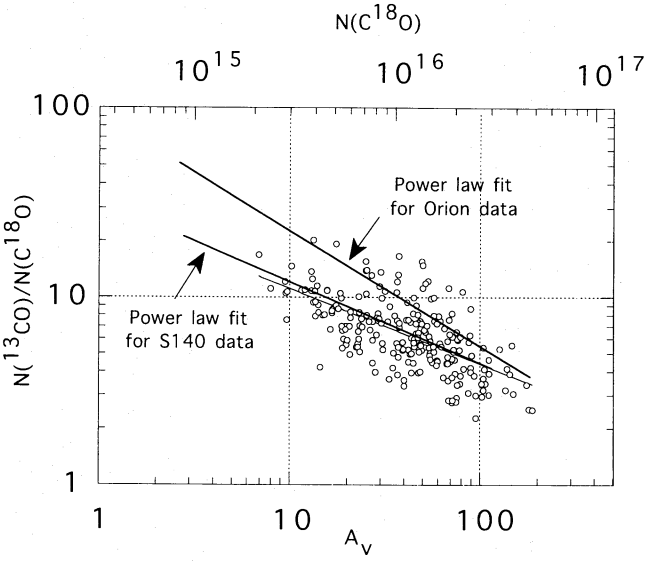

Fig. 2. Graph of $N(^{13}CO)/N(C^{18}O)$ plotted against visual extinction and $N(C^{18}O)$. The best fit power law is $N(^{13}CO)/N(C^{18}O) = 28A_v^{-0.4}$, with a correlation coefficient of 0.6. The fits obtained for the S140 and Orion Bright Bar regions are also plotted as bold lines (Minchin, White & Ward-Thompson 1995; White & Sandell 1995).

As expected, the highest values are observed towards positions with the lowest derived extinction, with $N(^{13}CO)/N(C^{18}O)$ exceeding the terrestrial value (5.5) for $A_v \leq 60$ magnitudes. In the outermost parts of the cloud, $A_v \sim 10$–20 magnitudes, the $N(^{13}CO)$ to $N(C^{18}O)$ ratio is largest, up to 20. This is consistent with the 1→0 and 2→1 line observations of Kutner et al. (1985). At the highest de-

rived extinction values the column density ratio falls below the canonical value of 5.5. This may be due to the higher optical depth of the ^{13}CO line, which becomes progressively more optically thick in the densest regions, whilst the C^{18}O remains optically thin. Although we have made an optical depth correction, this will become increasingly inadequate at the highest optical depths.

What is immediately apparent when comparing the three data sets is the fact that the $N(^{13}CO)$ to $N(C^{18}O)$ ratio observed towards the Bright Bar is systematically higher than observed towards either S140 or NGC 1977 over the same extinction range. This is reflected in the different power law fits, and is as high as a factor of 2.5 at the lowest extinctions ($A_v \leq 5$). The fact that the Bright Bar has a higher incident UV field ($\sim 10^5 G_o$) than S140 ($\sim 150 G_o$) or NGC 1977 ($\sim 360 G_o$) is suggestive that the increased fractionation is due to higher photodissociation of the optically thinner isotope, C^{18}O.

This is consistent with recent theoretical calculations of dense PDRs, which show that for more intense radiation fields, the lines of C^{18}O through which photodissociation occurs remain optically thin until deeper into the cloud (van Dishoeck, private communication). For a higher radiation field, C^{18}O is more rapidly dissociated than ^{13}CO for the same A_v. Whilst these results are suggestive, a sample of just three regions is insufficient to make firm conclusions. A large-scale observational study of numerous PDRs is required, with this data being closely linked to theoretical calculations of the expected degree of fractionation. It should also be noted that geometrical effects may be influencing the observed degree of fractionation at a given A_v (e.g. Hogerheijde et al. 1995).

4.2. N(CI)/N(CO) ratio

Figure 3 shows a plot of $N(CI)/N(CO)$ against visual extinction, as estimated from $N(C^{18}O)$. The CI column densities were derived using standard equations (e.g. Frerking et al. 1989), and have been corrected for optical depth in the same manner as the isotopic CO data (section 4.1). The optical depth of the CI line was found to be between 0.18 and 0.74. The excitation temperature is assumed to be the same as for the isotopic CO data.

There is a correlation between $N(CI)/N(CO)$ and visual extinction over the extinction range sampled by the 70 points (A_v ~10–105 mags.). The best fit power law is $N(CI)/N(CO) = 1.3 A_v^{-0.7}$, with a correlation coefficient of 0.8. This agrees well with the results for the Orion IRc2/Bright Bar and S140 regions ($N(CI)/N(CO) = 3 A_v^{-0.8}$, with a correlation coefficient of 0.8 and $N(CI)/N(CO) = 4.2 A_v^{-0.9}$, with a correlation coefficient of 1.0 respectively). The high values of $N(CI)/N(CO)$ at low extinction gives quantitative evidence for the increase in CI abundance in regions of high UV flux. The fact that the behaviour of the N(CI) to N(CO) ratio with extinction is quantitatively very similar in the S140, IRc2/Bright Bar and NGC 1977 regions suggests that, unlike the $N(^{13}CO)$ to $N(C^{18}O)$ ratio, it is insensitive to the intensity of the incident UV field. This is in broad agreement with recent modelling of PDRs (e.g. Hollenbach et al. 1991). An extensive dataset for several PDRs is required to allow quantitative conclusions about the behaviour of the N(CI) to N(CO) ratio with key physical parameters such as incident UV field, density and clumpy structure.

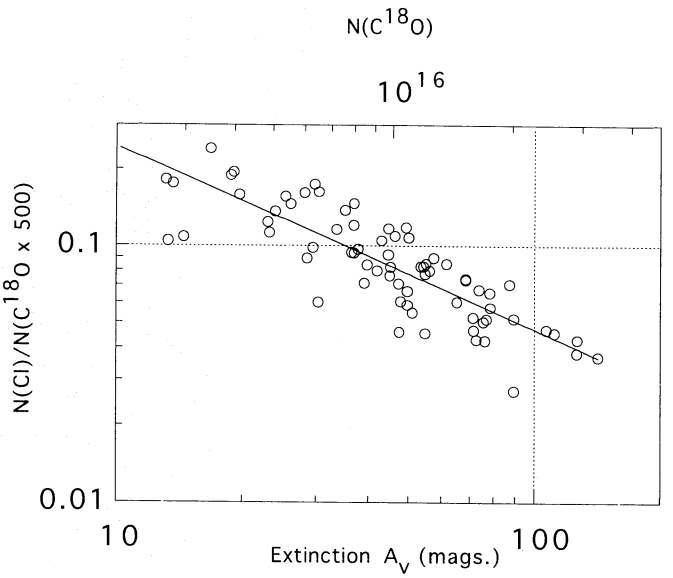

Fig. 3. Graph showing $N(CI)/N(CO)$ plotted against visual extinction and $N(C^{18}O)$. $N(CO)$ is derived from $N(C^{18}O)$, assuming a canonical abundance relative to CO of 500. The best fit power law is $N(CI)/N(CO) = 1.3 A_v^{-0.7}$, with a correlation coefficient of 0.8.

References

Le Bourlot J., Pineau des Forets G., Roueff E., Schilke P., 1993, ApJ 416, L87

van Dishoeck E. F., Black J. H., 1988 ApJ 334, 771

Frerking M. A., Langer W. D., Wilson R. W., 1982, ApJ 262, 590

Frerking M. A., Keene J., Blake G. A., Phillips T. G., 1989, ApJ 344, 311

Hogerheijde M. R., Jansen D. J., van Dishoeck E. F., 1995, A&A 294, 792

Hollenbach D. J., Takahashi T., Tielens A. G. G. M., 1991, ApJ 377, 192

Howe J. E., Jaffe D. T., Genzel R., Stacey G. J., 1991, ApJ 373, 158

Lada C. J., Lada E. A., Clemens D. P., Bally J., 1994, ApJ 429, 694

Keene J., Blake A., Phillips T. G., Huggins P. J., Beichman C. A., 1985, ApJ 299, 967

Kutner M. L., Evans N. J., Tucker K., 1976, ApJ 209, 452

Kutner M. L., Machnik D. E., Mead K. N., Evans N. J., 1985, ApJ 299, 351

Makinen P., Harvey P. M., Wilking B. A., Evans N. J., 1985, ApJ 299, 341

Minchin, N. R., White G. J., Ward-Thompson D., 1995, A&A in press

Prasad S. S., Tarafdar S. P., 1983, ApJ 267, 603

Stutzki J., Stacey G. J., Genzel R., Harris A. I., Jaffe D. T., Lugten J. B., 1988, ApJ 332, 379

Turner B. E., Xu L., Rickard L. J., 1982, ApJ 391, 158

White G. J., Padman R., 1991, Nat 354, 511

White G. J., Sandell G., 1995, A&A 299, 179

Wootten A., Phillips T. G., Beichman C. A., Frerking M., 1982, ApJ 256, L5

This article was processed by the author using Springer-Verlag LaTeX A&A style file 1990.